Diabatic states, nonadiabatic coupling, and the counterpoise procedure for weakly interacting open-shell molecules

Cite as: J. Chem. Phys. **148**, 094105 (2018); https://doi.org/10.1063/1.5013091
Submitted: 10 November 2017 . Accepted: 05 February 2018 . Published Online: 01 March 2018

Tijs Karman, Matthieu Besemer, Ad van der Avoird, and Gerrit C. Groenenboom

Diabatic states, nonadiabatic coupling, and the counterpoise procedure for weakly interacting open-shell molecules

Tijs Karman, Matthieu Besemer, Ad van der Avoird, and Gerrit C. Groenenboom[a)]
Theoretical Chemistry, Institute for Molecules and Materials, Radboud University, Heyendaalseweg 135, 6525 AJ Nijmegen, The Netherlands

(Received 10 November 2017; accepted 5 February 2018; published online 1 March 2018)

We study nonadiabatic coupling in systems of weakly interacting open-shell molecules which have nearly degenerate electronic states and hence significant nuclear derivative couplings. By comparison to numerically calculated nuclear derivatives of adiabatic electronic wave functions, we show that nonadiabatic couplings are represented accurately by diabatization using a recent multiple-property-based algorithm [T. Karman *et al.*, J. Chem. Phys. **144**, 121101 (2016)]. Accurate treatment of weakly interacting molecules furthermore requires counterpoise corrections for the basis-set superposition error. However, the generalization of the counterpoise procedure to open-shell systems is ambiguous. Various generalized counterpoise schemes that have been proposed previously are shown to be related through different choices for diabatization of the monomer wave functions. We compare these generalized counterpoise schemes and show that only two approaches accurately describe long-range interactions. In addition, we propose an approximate diabatization algorithm based on the asymptotic long-range interaction. This approach is appealingly simple to implement as it yields analytical expressions for the transformation to the diabatic representation. Finally, we investigate the effects of diabatizing intermolecular potentials on the nuclear dynamics by performing quantum scattering calculations for NO($X^2\Pi$)–H_2. We show that cross sections for pure rotational transitions are insensitive to diabatization. For spin-orbit inelastic transitions, asymptotic diabatization and multiple-property-based diabatization are in qualitative agreement, but the quantitative differences may be observable experimentally. *Published by AIP Publishing.* https://doi.org/10.1063/1.5013091

I. INTRODUCTION

Intermolecular interactions and molecular collisions in the gas phase are important in atmospheric chemistry, combustion, and astrochemistry. In these applications, radical species with unpaired electrons play a particularly important role. However, the theoretical treatment of collisions involving these open-shell species is complicated as their electronic states often are spatially degenerate. As an example, radicals such as NO and OH have an $X^2\Pi$ ground state,[1] which has two degenerate spatial components, e.g., Π_x and Π_y. In a collision complex, this leads to two electronic states that correlate to the degenerate monomer states asymptotically, i.e., for large separation between the colliding molecules. These electronic states are split only by the weak interaction with the collision partner and hence are nearly degenerate for all geometries. These states are coupled by the so-called nonadiabatic couplings that arise from the nuclear kinetic energy operator, which contains derivatives with respect to the nuclear coordinates, acting on electronic wave functions, which parametrically depend on the nuclear coordinates. Nonadiabatic couplings between nearly degenerate states can be significant or even divergent. Usually, nonadiabatic couplings are treated by diabatization: transforming to a diabatic basis, in which the derivative couplings vanish or are negligible, at the cost of introducing an off-diagonal electronic interaction.[2] The treatment of nonadiabatic couplings is also the subject of active research for reactive systems.[3–5] Here, however, we consider nonadiabatic coupling in systems consisting of weakly interacting open-shell molecules.

For open-shell diatomic molecules, diabatic states can be defined as products of complex-valued $\hat{L}_z$-adapted monomer states, i.e., monomer states which are eigenfunctions of the electronic orbital angular momentum along the molecular axis. Diabatization for open-shell molecules interacting with rare gas atoms is straightforward due to the planar symmetry in such systems.[6,7] For molecule-molecule systems, such symmetry is generally absent, but progress has been made in method development[8–14] that now enables the treatment of these systems.[15–19] In particular, some of the present authors have developed a multiple-property-based diabatization scheme specifically tailored towards weakly interacting open-shell molecules.[20] Strong nonadiabatic coupling is also encountered for complexes involving open-shell atoms[21–28] as well as for non-linear molecules such as the methane and benzene cations,[29–31] which also have spatially degenerate electronic states.

For the accurate treatment of weakly interacting molecules, it is essential to reduce the basis-set superposition error by the counterpoise (CP) procedure of Boys and Bernardi.[32] The generalization of this procedure to open-shell fragments is known to be ambiguous.[23,24,33] Several generalizations have been proposed in the literature, but to our knowledge these have never been compared critically. We find

[a)]Electronic mail: gerritg@theochem.ru.nl

that the long-range interaction, in particular, is highly sensitive to the counterpoise correction. We use the long-range interaction to gauge the accuracy of possible generalized counterpoise procedures. We show that the diabatic counterpoise correction of Alexander[33] and the approach of Kłos *et al.*[24] both lead to a smooth and correct R^{-n} dependence, with coefficients that are in agreement with separately computed monomer multipole moments. Other generalized correction schemes fail to describe the long-range interaction accurately.

Furthermore, we introduce a rotation-translation operator formalism to describe the electronic states of weakly interacting open-shell molecules as products of monomer wave functions. This permits a compact and rigorous derivation of the diabaticity of these states. We discuss various diabatization schemes. By comparison to numerically calculated derivative couplings of *ab initio* calculated adiabatic wave functions, we show that the recent multiple-property-based diabatization algorithm of Ref. 20 accurately represents nonadiabatic couplings.

We also propose an approximate diabatization algorithm based on the asymptotic long-range interaction. This algorithm is appealingly straightforward to implement as the asymptotic long-range interaction, and hence the transformation to the diabatic basis, is known analytically for many systems. This approach removes nonadiabatic couplings asymptotically, where they lead to singular derivative couplings, and is approximate in the short range, away from the degeneracy, where the dynamics are thought to become adiabatic and insensitive to residual derivative couplings. This approach has been proposed previously and applied in various contexts[26–28,34,35] but has never been compared to full diabatization by any algorithm. We show that the derivative couplings represented by asymptotic diabatization are qualitatively incorrect at short range but become increasingly more accurate at long range, which presumably is the region where nonadiabatic coupling is most significant in dynamical calculations. This idea is investigated by performing quantum scattering calculations for NO–H_2 collisions. In particular, we show that spin-orbit inelastic scattering is sensitive to diabatization. Although full multiple-property-based diabatization and approximate asymptotic diabatization are in qualitative agreement, the quantitative differences in the differential cross sections may be observable experimentally.[36–40]

This paper is organized as follows: Section II gives a brief introduction to nonadiabatic coupling, the Born-Oppenheimer approximation, and diabatization. In Sec. III, we give a definition of the diabatic states of a dimer of weakly interacting molecules, and we discuss the transformation to the diabatic representation. The elimination of derivative couplings between degenerate states is discussed rigorously in the Appendix. In Sec. III, we also review existing approaches for diabatization and propose a particularly simple, but approximate diabatization scheme based on the asymptotic long-range interaction. Section IV discusses generalizations of the counterpoise procedure to the open-shell case. Numerical results for the NO–H_2 system are given in Sec. V. We present a comparison between nuclear derivative couplings from *ab initio* calculated adiabatic wave functions, and the derivative couplings obtained from full multiple-property-based diabatization,[20] and the asymptotic diabatization scheme, proposed here. Furthermore, we investigate the accuracy of various counterpoise corrections. Finally, we consider the effects of diabatization on experimentally observable scattering cross sections. Concluding remarks are given in Sec. VI.

II. PRIMER ON NONADIABATIC COUPLING

The total wave function describing electrons and nuclei is expanded in electronic wave functions as

$$\Psi(\boldsymbol{r},\boldsymbol{R}) = \sum_i \phi_i(\boldsymbol{r};\boldsymbol{R})\chi_i(\boldsymbol{R}), \tag{1}$$

where the electronic wave functions, ϕ_i, are eigenstates of the electronic Hamiltonian,

$$\hat{H}_{\text{Electronic}}(\boldsymbol{R})\phi_i(\boldsymbol{r};\boldsymbol{R}) = \epsilon_i(\boldsymbol{R})\phi_i(\boldsymbol{r};\boldsymbol{R}). \tag{2}$$

The set $\{\phi_i\}$ is an orthonormal set of functions of the electronic degree of freedom, which parametrically depends on the nuclear coordinates. Inserting this ansatz into the time-independent Schrödinger equation yields nuclear Schrödinger equations for $\chi_i(\boldsymbol{R})$ where $\epsilon_i(\boldsymbol{R})$ plays the role of a potential.[41] The different electronic states are coupled by nonadiabatic first- and second-derivative couplings with respect to the nuclear coordinates, $\langle\phi_i|\nabla|\phi_j\rangle$ and $\langle\phi_i|\nabla^2|\phi_j\rangle$, respectively, which arise from the Born-Huang expansion employed in Ref. 41. Neglect of these nonadiabatic couplings leads to the adiabatic or Born-Oppenheimer approximation,[42] where $\Psi \approx \phi_0\chi_0$ and the dynamics take place on a single potential energy surface.

We note that the electronic wave functions, ϕ_i, need not be single-valued nor continuous twice-differentiable functions of $\boldsymbol{R}$, even though the total wave function, Eq. (1), does have this property. Single valuedness can be accounted for by geometric phases,[43] and singular derivatives can cancel exactly against derivatives of the nuclear wave functions, χ_i.

Going beyond the Born-Oppenheimer approximation, one can use a truncated expansion of the total wave function, Eq. (1). One then has the freedom to unitarily transform the electronic wave function without affecting the expansion,

$$\phi_j \to \psi_j = \sum_i \phi_i U_{i,j}. \tag{3}$$

In particular, one can attempt to find a transformation matrix, $\boldsymbol{U}(\boldsymbol{R})$, that eliminates the derivative couplings at the cost of introducing couplings by the off-diagonal diabatic potentials. This concept is called diabatization, and $\{\psi_j\}$ are diabatic states.

Eliminating derivative couplings by diabatization is not just a matter of convenience. Using the Hellmann-Feynman theorem, one can show that

$$\left\langle \phi_i \left| \frac{d}{dx} \right| \phi_j \right\rangle = \frac{\left\langle \phi_i \left| \frac{d\hat{H}}{dx} \right| \phi_j \right\rangle}{\epsilon_i - \epsilon_j}, \tag{4}$$

where x is any nuclear coordinate. If the numerator on the right-hand side does not vanish at an exact degeneracy, $\epsilon_i - \epsilon_j = 0$, or conical intersection, the derivative couplings are singular. These singular derivative couplings cannot be treated in numerical nuclear dynamics calculations. Hence, diabatization

is essential for electronic states that are nearly degenerate, but coupling to energetically well separated states can be neglected safely. The accuracy of the latter approximation should be comparable to that of the Born-Oppenheimer approximation for closed-shell systems.

III. DIMER DIABATIC STATES

The electronic wave function for two non-interacting diatomic molecules can be written as[44]

$$|\psi^{(A)}\psi^{(B)}\rangle = \hat{\mathcal{A}}\left[\hat{\mathcal{T}}(\boldsymbol{R}_A)\hat{\mathcal{R}}(\alpha_A,\beta_A,\gamma_A)\,|\,\psi^{(A)}\rangle\right] \otimes \left[\hat{\mathcal{T}}(\boldsymbol{R}_B)\hat{\mathcal{R}}(\alpha_B,\beta_B,\gamma_B)\,|\,\psi^{(B)}\rangle\right]. \quad (5)$$

This wave function describes two molecules, $X = A, B$, with centers of mass $\boldsymbol{R}_X$, in electronic state $\psi^{(X)}$, and oriented at z-y-z Euler angles α_X, β_X, and γ_X. For the case of a linear molecule, X, the angles β_X and α_X are the spherical polar angles and $\gamma_X = 0$. The operators

$$\begin{aligned}\hat{\mathcal{R}}(\alpha,\beta,\gamma) &= e^{-\alpha\hat{j}_z}e^{-\beta\hat{j}_y}e^{-\gamma\hat{j}_z},\\ \hat{\mathcal{T}}(\boldsymbol{R}) &= e^{-i\boldsymbol{R}\cdot\hat{\boldsymbol{p}}}\end{aligned} \quad (6)$$

are the rotation and translation operators, respectively, where $\hat{\boldsymbol{j}}$ and $\hat{\boldsymbol{p}}$ are the electronic angular and linear momentum operators. The operator $\hat{\mathcal{A}}$ antisymmetrizes the electronic wave function with respect to the exchange of any two electrons. In the Appendix, we develop the rotation-translation operator formalism for the description of the electronic states of Eq. (5). This formalism permits a compact derivation of the diabaticity of these wave functions, i.e., these wave functions have vanishing derivative couplings with respect to the center of mass motion of either molecule, and rotational nonadiabatic couplings can be eliminated by a convenient choice of rotational wave functions.

In the literature, the equivalent of Eq. (5) is typically implicitly dependent on the nuclear coordinates, where the electronic monomer wave functions are defined in molecule-fixed frames.[6,7] This leads to equations that are valid only within a certain implicitly defined coordinate frame. Furthermore, one formally cannot uniquely define electronic wave functions for half-integer spin by attaching them to molecule-fixed frames because under rotations the frame transforms according to SO(3), whereas the rotation of half-integer spin is described by SU(2). The wave function for half-integer spin changes sign under a 2π rotation and hence cannot be defined in a frame that is invariant to such rotations.

For weakly interacting diatomic molecules, the adiabatic electronic wave functions can be approximated by linear combinations of antisymmetrized products of monomer wave functions

$$|\Psi_a^{(\text{Adiabatic})}\rangle = \sum_{i,j}|\psi_i^{(A)}\psi_j^{(B)}\rangle\, U_{i,j;a}. \quad (7)$$

In *ab initio* calculations, one directly obtains the adiabatic wave functions, $|\Psi_a^{(\text{Adiabatic})}\rangle$, as eigenstates of the electronic Hamiltonian. As the expansion coefficients $U_{i,j;a}$ may vary rapidly with nuclear geometry, these adiabatic electronic wave functions may have appreciable—or even singular—nonadiabatic couplings, rendering them unsuitable for subsequent dynamical calculations. This issue is remedied by transforming to the diabatic representation, Eq. (5), using a transformation $\boldsymbol{U}$, with elements $U_{i,j;a}$. The problem of actually determining this transformation matrix is called diabatization and some approaches are discussed in Subsections III A–III D.

At this point, it is worthwhile to specialize the discussion to the NO–H_2 system, considered below: an open-shell diatomic molecule in a $^2\Pi$ electronic state interacting with a closed-shell $^1\Sigma_g^+$ diatom. In this case, there are two diabatic states, $\{|\Pi_{+1}\rangle, |\Pi_{-1}\rangle\}$, using the short-hand notation $|\Pi_\alpha\rangle \equiv |^2\Pi_\alpha\,{}^1\Sigma_g^+\rangle$, and two corresponding adiabatic states. These are related by

$$\begin{aligned}\left[|\Psi_1\rangle,\ |\Psi_2\rangle\right] &= \left[|\Pi_x\rangle,\ |\Pi_y\rangle\right]\begin{bmatrix}\cos(\varphi) & \sin(\varphi)\\ -\sin(\varphi) & \cos(\varphi)\end{bmatrix}\\ &= \left[|\Pi_{+1}\rangle, |\Pi_{-1}\rangle\right]\frac{1}{2}\sqrt{2}\begin{bmatrix}-1 & i\\ 1 & i\end{bmatrix}\begin{bmatrix}\cos(\varphi) & \sin(\varphi)\\ -\sin(\varphi) & \cos(\varphi)\end{bmatrix}\\ &= \left[|\Pi_{+1}\rangle,\ |\Pi_{-1}\rangle\right]\boldsymbol{U}(\varphi),\end{aligned} \quad (8)$$

which parameterizes the 2×2 diabatic-to-adiabatic transformation matrix, $\boldsymbol{U}$, by a single mixing angle, φ. This considerably simplifies the discussion. The diabatic potential energy matrix is obtained by transforming the *ab initio* computed adiabatic potentials as

$$\begin{aligned}\boldsymbol{V}^{(\text{Diabatic})} &= \boldsymbol{U}(\varphi)\boldsymbol{V}^{(\text{Adiabatic})}\boldsymbol{U}(\varphi)^\dagger\\ &= \begin{bmatrix}\epsilon & \frac{\Delta E}{2}\exp(2i\varphi)\\ \frac{\Delta E}{2}\exp(-2i\varphi) & \epsilon\end{bmatrix},\end{aligned} \quad (9)$$

where

$$\boldsymbol{V}^{(\text{Adiabatic})} = \begin{bmatrix}\epsilon - \frac{\Delta E}{2} & 0\\ 0 & \epsilon + \frac{\Delta E}{2}\end{bmatrix}, \quad (10)$$

that is, ϵ is the mean adiabatic energy and $\Delta E \geq 0$ is the adiabatic energy splitting. This motivates a crude approximation to diabatization: If one can neglect the energy splitting and assume

$$\Delta E = 0, \quad (11)$$

the diabatic potential energy matrix is completely independent of the mixing angle, φ, and determined only by the average adiabatic potential. As is shown numerically below, this may be reasonable for some dynamical processes that are insensitive to the off-diagonal potential, whereas it leads to qualitatively wrong results for spin-orbit changing transitions of NO, for example.[7]

A. Integration of derivative couplings

The nonadiabatic coupling between two adiabatic states is given by

$$\begin{aligned}\langle\Psi_1^{(A)}|\frac{d}{dx}|\Psi_2^{(A)}\rangle &= \sum_{d_i}\langle\Psi_1^{(A)}|\Psi_{d_i}^{(D)}\rangle\langle\Psi_{d_i}^{(D)}|\\ &\quad\times\frac{d}{dx}\left[\sum_{d_j}|\Psi_{d_j}^{(D)}\rangle\langle\Psi_{d_j}^{(D)}|\Psi_2^{(A)}\rangle\right]\\ &= \sum_d U_{d,1}^*\frac{d}{dx}U_{d,2} = \frac{d\varphi}{dx},\end{aligned} \quad (12)$$

where φ is the mixing angle defined in Eq. (8) and x is any nuclear coordinate. Thus, one can obtain the mixing angle by integrating nuclear derivative couplings

$$\varphi(x) = \varphi(x_0) + \int_{x_0}^{x} \langle \Psi_1 | \frac{d}{dx'} | \Psi_2 \rangle dx', \tag{13}$$

where $x = x_0$ is a reference geometry at which the mapping between adiabatic and diabatic states, and therefore the mixing angle, is known. Equation (12) neglects the coupling to states that are not included in the diabatic model. These states should be energetically well-separated from the states of interest and hence are not expected to cause singular nonadiabatic couplings. The accuracy of this approximation is comparable to the Born-Oppenheimer approximation for closed-shell fragments.

This approach also exposes a problem in more than one dimension, i.e., more than one nuclear coordinate.[45] Here, one has a vector of derivative couplings which satisfies

$$\langle \Psi_1 | \nabla | \Psi_2 \rangle = \nabla \varphi, \tag{14}$$

which has a solution for the mixing angle, φ, if and only if the left-hand size had zero curl, that is, if

$$\frac{\partial}{\partial x_i} \left[\langle \Psi_1 | \frac{\partial}{\partial x_j} | \Psi_2 \rangle \right] - \frac{\partial}{\partial x_j} \left[\langle \Psi_1 | \frac{\partial}{\partial x_i} | \Psi_2 \rangle \right] = 0. \tag{15}$$

This is not generally the case, which means that the derivative coupling cannot be transformed away completely, and *strictly* diabatic states do not exist in more than one degree of freedom. In this case, only the curl-free part of the derivative coupling can be removed by a transformation to *quasi*-diabatic states.[45] The diabatic states discussed in this paper are thus in fact quasi-diabatic. The transformation to quasi-diabatic states can, however, still eliminate the singular part of the derivative couplings at a conical intersection and in principle represent derivative couplings to good accuracy. The residual derivative couplings, which cannot be transformed away, are due to coupling to energetically well-separated states that are not contained in the diabatic model and hence are expected to be non-singular and of comparable order to those neglected in the Born-Oppenheimer approximation for closed-shell systems.

The nonexistence of a strictly diabatic basis has motivated various alternative diabatization schemes, which should still eliminate the problematic singular part of the derivative couplings but have the advantage of bypassing the *ab initio* computation of derivative couplings, which are otherwise required on a dense grid for numerical integration. Below, we discuss and propose such approximate diabatization schemes.

B. Symmetry-based diabatization

It is mentioned above that there exist reference geometries at which the mapping between adiabatic and diabatic states, or the mixing angle, is known. This is typically the case for high-symmetry geometries. For the NO–H_2 example in mind here, this occurs for geometries with a plane of reflection symmetry containing the NO bond axis, where there is direct correspondence between the adiabatic states carrying A' and A'' irreducible representations of the C_s point group and the diabatic $|\Pi_x\rangle$ and $|\Pi_y\rangle$ states. This symmetry-determined transformation is used for diatom(Π)–atom(^1S) systems[6] which always have reflection symmetry in the triatomic plane. For diatom(Π)–diatom($^1\Sigma$) systems, this approach has been applied to NO–H_2[16] and OH–H_2,[15] where the geometries were restricted to either coplanar or with the H_2 molecule perpendicular to the plane containing NO and the H_2 center of mass. Symmetry-based diabatization is straightforward but severely restricts the sampling of geometries, such that it is applicable only to weakly anisotropic systems, such as those involving H_2 molecules, but still fails for CH($^2\Pi$)–H_2,[46] for example.

C. Property-based diabatization

A straightforward way to determine the transformation matrix is by directly inspecting the *ab initio* wave functions and comparing these to the diabatic wave functions of Eq. (5). This can be done either by maximizing overlap with reference wave functions[8,9,11–13] or by "manual" inspection of the wave function.[10,47] In order to avoid tedious manual inspection of the *ab initio* wave functions, property-based diabatization algorithms have been developed[10,14,20] that furthermore have the advantage of direct applicability irrespective of the level of theory at which adiabatic wave functions—and their properties—were computed.

One approach is to require the transformed adiabatic properties to be smooth functions of the nuclear coordinates such that the transformed wave functions also become smooth and hence diabatic. The dipole and quadrupole (DQ) method of Ref. 14 accomplishes this by extremizing a functional involving elements of the dipole and quadrupole tensors. In Ref. 10, a selected *transition* property is diagonalized, which diabatizes as the resulting eigenvalues of the dipole component typically become smoother functions of the nuclear coordinates.

In Ref. 20, some of the present authors have presented a different type of property-based diabatization, where one does not require transformed properties to be smooth by construction, but rather one looks for a mapping between adiabatic and diabatic properties which are both assumed to be known. That is, one calculates properties adiabatically, from *ab initio* wave functions, as well as diabatically, from the model wave functions of Eq. (5), and subsequently determines a similarity transformation that relates these properties. Advantages are that this method can be applied directly to any number of states, includes any number of properties on equal footing, and involves only standard matrix operations of low dimensions. The disadvantage is that it requires knowledge of model diabatic wave functions, such as Eq. (5). This equation applies generally to van der Waals molecules only. This multiple-property-based diabatization algorithm is applied to NO–H_2 below, in Sec. V.

D. Asymptotic diabatization

Here, we propose an approximate diabatization scheme for van der Waals molecules with spatially degenerate fragments, namely, to use the asymptotic form of the transformation, $\boldsymbol{U}$, as the distance between the fragments tends to infinity, $R \to \infty$. The motivation for this approximation is that nonadiabatic couplings are most significant where adiabatic

states are close in energy, so one will want to remove the nonadiabatic coupling asymptotically, where the adiabatic states become degenerate. At short separation, there will be residual derivative couplings, but these should be less significant to the dynamics as the degeneracy of the adiabatic states has been lifted by the short-range interaction. This idea has been applied also for the interaction between two open-shell atoms in degenerate electronic states,[26–28,48] but to our knowledge, its accuracy has not yet been compared to any numerical diabatization method. Similar approximations have also been made for Jahn-Teller systems,[34,35] where the transformation to diabatic states was determined from the lowest order in a Taylor expansion of the interaction around a degeneracy.

The asymptotic transformation between the adiabatic and diabatic representations can be obtained by diagonalizing the asymptotic interaction in the diabatic representation. The asymptotic interaction is known analytically, in many cases, except for an overall scaling. Derivations of the long-range interaction between open-shell diatomic molecules are presented in Ref. 47 and the supplementary material of Ref. 1. For example, for a Π-state diatomic molecule interacting with a closed-shell Σ-state molecule, the asymptotic form of the off-diagonal interaction is given by the quadrupole-dipole coupling,

$$\langle \Pi_{+1}|\hat{V}_{\text{asymp}}|\Pi_{-1}\rangle = \frac{c_4}{R^4}\sum_{M=-1}^{1} D^{(2)*}_{M,2}(0,\theta_A,0) \times D^{(1)*}_{-M,0}(\phi,\theta_B,0)\langle 2,M,1,\ -M|3,0\rangle. \tag{16}$$

If molecule B is homonuclear and hence has no dipole moment, the asymptotic off-diagonal interaction is given by the quadrupole-quadrupole coupling,

$$\langle \Pi_{+1}|\hat{V}_{\text{asymp}}|\Pi_{-1}\rangle = \frac{c_5}{R^5}\sum_{M=-2}^{2} D^{(2)*}_{M,2}(0,\theta_A,0) \times D^{(2)*}_{-M,0}(\phi,\theta_B,0)\langle 2,M,2,\ -M|4,0\rangle. \tag{17}$$

In the above equation, we have chosen the z axis parallel to the intermolecular axis and molecule A in the xz-plane. The eigenvectors are independent of both the separation, R, and the long-range coefficient, c_n, although the ordering of the adiabatic states depends on the sign of c_n. The transformation between the adiabatic and diabatic representations, parameterized for the two-state case by a single angle, φ, defined in Eq. (8), can be obtained from the asymptotic interaction analytically

$$\varphi = \frac{1}{2}\text{Arg}\left(\langle \Pi_{+1}|\hat{V}_{\text{asymp}}|\Pi_{-1}\rangle\right), \tag{18}$$

where Arg is the complex argument.

We note that, in principle, it may happen that the leading interaction does not lift the degeneracy of the adiabatic states, for example, because $\langle \Pi_{+1}|\hat{V}_{\text{asymp}}|\Pi_{-1}\rangle$ vanishes for certain orientations. In such cases, one could include the next-to-leading term. Inclusion of the next-to-leading term could also be included to improve the accuracy, and in order to include radial derivative couplings, which vanish for the R-independent mixing angle obtained from the asymptotic interaction. However, this is not attempted here as it considerably complicates the theory; the resulting mixing angle would depend on the relative strength of long-range interactions, and both first-order electrostatics and second-order dispersion contribute at order R^{-6}. Asymptotic diabatization is considered here as an appealingly simple approach to diabatization, yielding the transformation between the adiabatic and diabatic representations analytically, without prior knowledge of the strength of the long-range interaction. We stress that the presented asymptotic method is different from the property-based methods, discussed in Sec. III C, and this can be applied independently.

The asymptotic method cannot be applied if there is no analytically known long-range interaction, for example, where two diabatic states correspond to different monomer spin or charge states.

IV. COUNTERPOISE CORRECTION

Interaction energies are defined as the difference of the total energies of the complex and its separate fragments,

$$V(\boldsymbol{R}) = E^{(AB)}(\boldsymbol{R}) - E^{(A)} - E^{(B)}, \tag{19}$$

where $\boldsymbol{R}$ schematically denotes the complete specification of the nuclear geometry of the complex. In practice, calculations usually employ the so-called counterpoise (CP) procedure of Boys and Bernardi,[32] which entails evaluation of all energies in the dimer-centered one-electron basis set. This also includes *ghost* functions centered on molecule B when computing $E^{(A)}$, and vice versa. The interaction is thus computed as

$$V(\boldsymbol{R}) = E^{(AB)}(\boldsymbol{R}) - E^{(A)}(\boldsymbol{R}) - E^{(B)}(\boldsymbol{R}), \tag{20}$$

where the monomer energies in the dimer basis set are now weakly dependent on the geometry of the complex, through the positions of the ghost orbitals. This procedure reduces the basis-set superposition error and improves the accuracy of the computed interaction due to systematic cancellation of errors associated with the truncated one-electron basis set.[32]

If one wishes to extend the CP procedure of Boys and Bernardi to open-shell systems, the situation becomes slightly more complicated as multiple electronic states may be involved. For simplicity, we again consider the two-state case for NO–H_2. In this case, the interaction as well as the energies of the complex AB and monomer A (NO) is represented by 2×2 matrices. Not only the monomer adiabatic energies but also the monomer mixing angle, $\varphi^{(A)}$, between monomer adiabatic and diabatic states are $\boldsymbol{R}$ dependent due to the ghost orbital basis. The mixing angle for the monomer calculation, $\varphi^{(A)}$, can be obtained by the same diabatization procedure as is employed for the dimer calculation. The mixing angles obtained in complex and monomer calculations will generally be different, $\varphi^{(A)} \neq \varphi^{(AB)}$.

In 1993, Alexander introduced a generalized counterpoise correction, which we refer to as the diabatic CP correction.[33] In this counterpoise scheme, Eq. (20) is applied to all diabatic potentials. This can be written compactly in matrix notation as

$$\boldsymbol{V}(\boldsymbol{R}) = \boldsymbol{E}^{(AB)}(\boldsymbol{R}) - \boldsymbol{E}^{(A)}(\boldsymbol{R}) - E^{(B)}(\boldsymbol{R})\boldsymbol{I}_{2\times 2}, \tag{21}$$

where the interaction, $\boldsymbol{V}$, energy of the complex AB, $\boldsymbol{E}^{(AB)}$, and monomer energy, $\boldsymbol{E}^{(A)}$, are all evaluated in the diabatic representation.

Later, further generalizations have been proposed. In particular, it has been stated that it would be preferable to perform the CP correction at an adiabatic level.[24] We define the adiabatic CP correction[33] as applying Eq. (20) to each adiabatic state, i, that is,

$$V_i(\boldsymbol{R}) = E_i^{(AB)}(\boldsymbol{R}) - E_i^{(A)}(\boldsymbol{R}) - E^{(B)}(\boldsymbol{R}). \tag{22}$$

This yields the adiabatic interaction matrix, which is subsequently diabatized.

To the best of our knowledge, the performance of various generalized CP schemes has never been compared. It is not clear *a priori* which generalized CP scheme is the most appropriate, nor whether systematic differences in their performance even exist. Below, we summarize some of the possible generalizations,[23,24,33] show how they are related, and test their numerical performance in Sec. V B.

In the diabatic CP correction scheme of Alexander,[33] all total energy matrices in Eq. (21), $\boldsymbol{E}$, are evaluated in the diabatic representation. In order to make the connection with the adiabatic CP scheme more apparent, we may transform Eq. (21) to the adiabatic representation for the dimer calculation. This is accomplished by transforming with $\boldsymbol{U}^\dagger[\varphi^{(AB)}]$. In the adiabatic representation, the energy matrix $\boldsymbol{E}^{(AB)}$ is diagonal. The matrix $\boldsymbol{E}^{(A)}$ is obtained by transforming the monomer adiabatic energies with $\boldsymbol{U}^\dagger[\varphi^{(AB)}]\boldsymbol{U}[\varphi^{(A)}]$, which yields

$$\begin{aligned}\boldsymbol{E}^{(A)}(\boldsymbol{R}) &= \begin{bmatrix} \cos(\Delta\varphi) & \sin(\Delta\varphi) \\ -\sin(\Delta\varphi) & \cos(\Delta\varphi) \end{bmatrix} \\ &\times \begin{bmatrix} \epsilon^{(A)} - \frac{1}{2}\Delta E^{(A)} & 0 \\ 0 & \epsilon^{(A)} + \frac{1}{2}\Delta E^{(A)} \end{bmatrix} \\ &\times \begin{bmatrix} \cos(\Delta\varphi) & -\sin(\Delta\varphi) \\ \sin(\Delta\varphi) & \cos(\Delta\varphi) \end{bmatrix} \\ &= \epsilon^{(A)}\, \boldsymbol{I}_{2\times 2} + \frac{1}{2}\Delta E^{(A)} \begin{bmatrix} -\cos(2\Delta\varphi) & \sin(2\Delta\varphi) \\ \sin(2\Delta\varphi) & \cos(2\Delta\varphi) \end{bmatrix}. \end{aligned} \tag{23}$$

In the above equation, $\epsilon^{(A)}$ is the mean adiabatic energy and $\Delta E^{(A)}$ is the splitting of the adiabatic energies obtained in the calculation for monomer A. The phase angle $\Delta\varphi = \varphi^{(AB)} - \varphi^{(A)}$ is the mixing angle between the adiabatic representations of the complex AB and monomer calculations. This diabatic CP correction coincides with the adiabatic correction if $\Delta\varphi = 0$ and differs otherwise.

The partitioning of the CP correction in the last line of Eq. (23) is insightful as the first term is a multiple of the unit matrix, affecting only the trace, and the second term is traceless. Because the two diagonal potentials, corresponding to $\Lambda_A = \pm 1$, are equal, the first term represents a CP correction to only the diagonal potential, and the second one contributes only to the off-diagonal or coupling potential. The first term is invariant under unitary transformations, which means that for the diagonal potential it does not matter in which representation one performs the CP correction, and all generalized CP methods mentioned in this section should yield exactly the same result.

The CP correction to the off-diagonal potential is sensitive to the choice of representation in which the monomer energies are evaluated, and some options found in the literature are summarized here.

- Diabatic correction
  The diabatic correction of Alexander is equivalent to using Eq. (21), or Eq. (23) with $\varphi^{(A)}$ and $\varphi^{(AB)}$ evaluated using the same diabatization scheme; see Ref. 33.
- Mean correction
  The mean CP correction—averaged over the contributing monomer states—was used in Ref. 44. From the analysis presented above, it is seen that using only the mean adiabatic energy, and neglecting the splitting, will give a CP correction for the diagonal potentials only. This corresponds to Eq. (23) with $\Delta E^{(A)} = 0$.
- Adiabatic correction
  Correcting using the adiabatic energies is equivalent to using Eq. (23) with $\Delta\varphi = 0$, i.e., assuming that the adiabatic representation in the monomer and complex calculations coincide.[33]
- Reverse adiabatic correction
  The reverse adiabatic correction amounts to using Eq. (23) assuming $\Delta\varphi = \frac{1}{2}\pi$, meaning that the adiabatic states in the monomer and complex calculations are in reverse order. This is motivated by Alexander as the lowest adiabatic state in the monomer calculations and is the state that is more stabilized by the ghost basis functions of the second molecule, i.e., where the open-shell electron is closer to the second molecule. For the complex, this would typically be the more repulsive state and hence the order of the states should be reversed.[33]
- Correction of Kłos *et al.*
  In the correction of Ref. 24—which was originally motivated as an adiabatic CP correction—the difference in mixing angle is determined and used to transform the monomer energies to the dimer adiabatic representation but subsequently neglects any off diagonal elements. This amounts to assuming $\sin(2\Delta\varphi) = 0$ in Eq. (23), but it is different from the adiabatic correction as it does *not* assume $\cos(2\Delta\varphi) = 1$. Therefore, this method is also capable of describing the situation where the order of the adiabatic states is reversed if $\Delta\varphi \approx \frac{1}{2}\pi$. In case the adiabatic states are strongly mixed, e.g., $\Delta\varphi \approx \frac{1}{4}\pi$, the correction to the off-diagonal potential vanishes smoothly as $\cos(2\Delta\varphi)$.

V. NUMERICAL RESULTS FOR NO–H_2

Here, we present numerical results for the interaction between NO($X^2\Pi$) and H_2. We calculated orbitals using a two-state two-configuration MCSCF calculation, state averaged with equal weights, with the single unpaired electron in two orbitals. This yields single-determinant descriptions of both states of the NO–H_2 complex, using pseudo-canonical orbitals, which were used as reference functions in partially spin-restricted coupled cluster calculations with single and double

excitations and perturbative triples [CCSD(T)]. The adiabatic CCSD(T) energies were transformed to the diabatic representation, using the recent multiple-property-based method of Ref. 20, with quadrupole moments and angular momenta calculated for the reference wave functions. Diabatization for the monomer calculations, encountered in the diabatic CP correction, was performed identically. All calculations were performed using MOLPRO using an aug-cc-pVQZ basis set.[49] The applicability of RCCSD(T) to these nearly degenerate electronic states was monitored throughout by comparing the excitation energy, i.e., the energy splitting of the two states, to results of multi-reference configuration interaction (MRCI) calculations. Additional computational details and routines for evaluation of the potential can be found in Ref. 17.

Below, and without loss of generality, we choose the intermolecular axis as the z axis and the NO molecule in the xz-plane. Hence, the geometry as defined through Eq. (5) is given by $\boldsymbol{R}_A = -\frac{m_{H_2}}{m_{NO}+m_{H_2}} R\hat{z}$, $\boldsymbol{R}_B = \frac{m_{NO}}{m_{NO}+m_{H_2}} R\hat{z}$, $\beta_A = \theta_{NO}$, $\beta_B = \theta_{H_2}$, $\alpha_B = \phi$, and $\alpha_A = \gamma_A = \gamma_B = 0$, where m_{NO} and m_{H_2} are the monomer masses, and R, θ_{NO}, θ_{H_2}, and ϕ are the Jacobi coordinates. The monomer bond lengths are kept fixed at $r_{NO} = 2.1803\ a_0$ and $r_{H_2} = 1.448\ a_0$ throughout.[16]

A. Nonadiabatic coupling

We first explicitly show that multiple-property-based diabatization[20] accurately represents the nonadiabatic derivative couplings. To this end, we calculate the derivative couplings both numerically and from diabatization. We numerically obtain derivative couplings, $\langle \Psi_1 | \frac{d}{dx} | \Psi_2 \rangle$, from the adiabatic MCSCF reference wave functions, which were computed as described above, in MOLPRO using the DDR utility.[49] The nuclear coordinate, x, represents any of the Jacobi coordinates, $x \in \theta_{NO}, \theta_{H_2}, \phi, R$. Briefly, the DDR procedure computes derivative couplings using finite differences from adiabatic wave functions computed at the geometry of interest and for finite displacements, Δx, along the nuclear coordinate x. The accuracy of the finite-differences approach was monitored throughout, and typical displacements were in the order of 0.1° for the angular coordinates, and ΔR was between 0.001 and 0.1 a_0. The derivative couplings as represented by diabatization were obtained from the diabatic-to-adiabatic transformation matrix, $\boldsymbol{U}$, using Eq. (12). We explicitly evaluated the couplings for transformation matrices determined using multiple-property-based diabatization[20] and for the asymptotic diabatization proposed here.

Figure 1 shows the derivative couplings between the lower and upper adiabatic states as a function of θ_{NO}, for various values of R, and an otherwise fixed geometry defined by the Jacobi angles $\theta_{H_2} = 90°$ and $\phi = 45°$. The solid lines represent the results of finite differences calculations, which are reproduced accurately by the results of the multiple-property-based diabatization algorithm of Ref. 20, shown as the plus-sign markers: The couplings obtained differ by less than 0.5% of the maximum coupling for all geometries shown and are difficult to distinguish visually. A notable exception occurs for the coupling due to d/dR at the shortest distances, near $\theta_{NO} = 130°$, where the coupling is small in absolute sense, and both methods predict a zero-crossing at slightly displaced geometries, as is seen more clearly in Fig. 2, in a similar plot as a function of R.

Figure 1 furthermore shows striking differences between nonadiabatic couplings for various values of R. For large R, the nonadiabatic couplings do approach the result obtained by asymptotic diabatization, but even at $R = 25\ a_0$, significant differences are observed. In Sec. V C, we further investigate the accuracy of the proposed asymptotic diabatization in dynamical calculations.

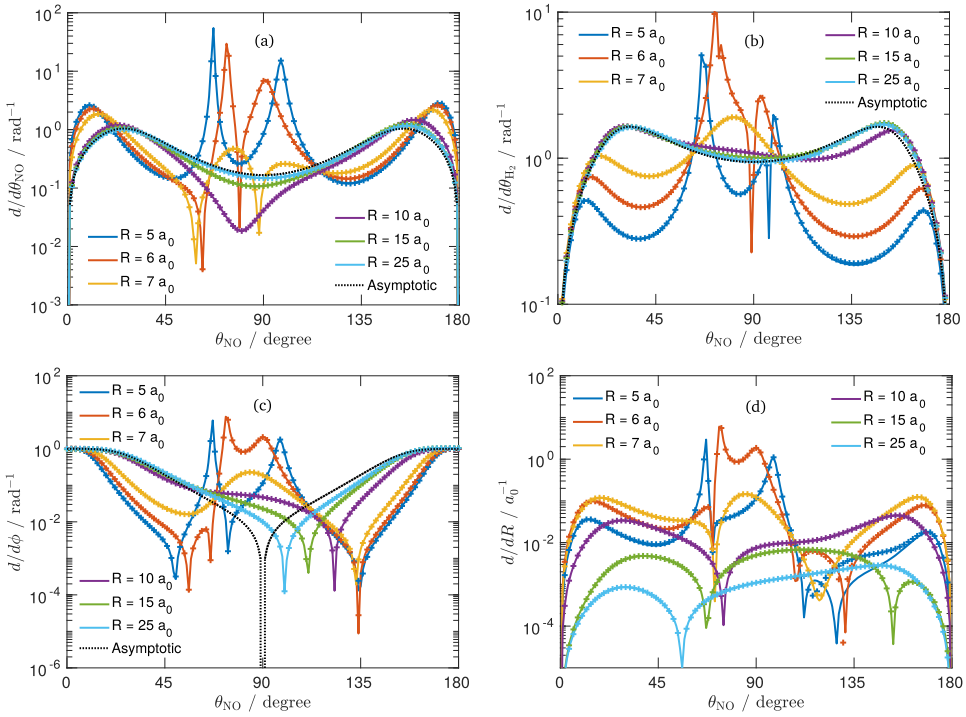

FIG. 1. Nonadiabatic derivative couplings as a function of θ_{NO}, for various values of R (color coded), and an otherwise fixed geometry, defined by $\theta_{H_2} = 90°$ and $\phi = 45°$. (a)–(d) show the couplings due to $d/d\theta_{NO}$, $d/d\theta_{H_2}$, $d/d\phi$, and d/dR, respectively. These are calculated numerically from adiabatic electronic wave functions at the MCSCF level (solid lines), from the diabatic wave functions as obtained by multiple-property-based diabatization (plus markers), or from asymptotic diabatization (black dotted line). Asymptotic diabatization predicts vanishing nonadiabatic couplings due to d/dR, which are not indicated.

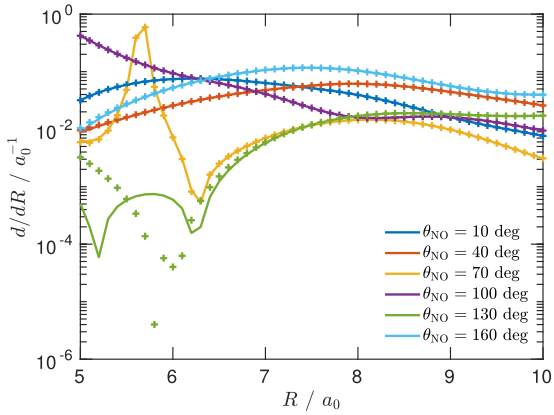

FIG. 2. Nonadiabatic coupling due to d/dR, as a function of R, for various values of θ_{NO} (color coded), and an otherwise fixed geometry, defined by $\theta_{H_2} = 90°$ and $\phi = 45°$. Couplings are calculated numerically from adiabatic electronic wave functions at the MCSCF level (solid lines) and from the diabatic wave functions as obtained by multiple-property-based diabatization (plus markers).

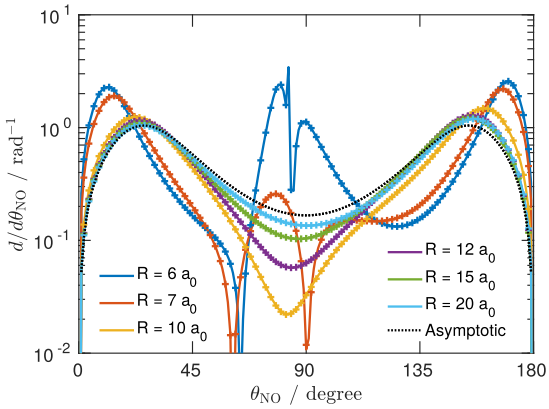

FIG. 3. Nonadiabatic derivative couplings due to $d/d\theta_{NO}$ as a function of θ_{NO}, for various values of R (color coded), and an otherwise fixed geometry, defined by $\theta_{H_2} = 90°$ and $\phi = 45°$. These are calculated numerically from adiabatic electronic wave functions at the MCSCF level (solid lines), from the diabatic wave functions as obtained by multiple-property-based diabatization (plus markers), or from asymptotic diabatization (black dotted line).

We have repeated the calculations of nonadiabatic couplings presented above at the complete active space self-consistent field (CASSCF) level of theory, employing a larger full valence active space. The resulting nonadiabatic couplings due to $d/d\theta_{NO}$ are shown in Fig. 3. The nonadiabatic couplings at the full valence CASSCF level of theory are somewhat different from those of the two-configuration MCSCF, in particular at shorter distances. However, the agreement between the results of the multiple-property-based diabatization algorithm and the couplings as computed by finite differences using Molpro remains excellent.

B. Counterpoise correction and long-range interactions

Here, we compare different methods for performing the counterpoise correction. To this end, we consider the long-range interaction. Because the long-range interaction is weak in absolute sense, it is sensitively dependent on such corrections. Nevertheless, it is relevant for the scattering dynamics, and the correct long-range is known from perturbation theory and separately computed multipole moments, which makes it a convenient test.

Figure 4 shows the expansion coefficients for the L_A, L_B, L = 2, 2, 4 and 3, 2, 5 terms of the diagonal potential, which should asymptotically approach the quadrupole-quadrupole and octupole-quadrupole interactions, respectively. These expansion coefficients have been multiplied by R^5 and R^6, respectively, such that they should become constant in the limit as $R \to \infty$. The expected limit is

$$V_{L_A,L_B,L} = \delta_{L_A+L_B,L}(-1)^{L_B}\begin{pmatrix} 2L \\ 2L_A \end{pmatrix}^{1/2} \times \langle \psi'^{(A)} | Q_{L_A,K_A} | \psi^{(A)} \rangle \langle \psi'^{(B)} | Q_{L_B,0} | \psi^{(B)} \rangle R^{-L-1}, \quad (24)$$

where $K_A = 0$ or 2 for diagonal and off-diagonal potentials, respectively, and $\langle \psi'^{(X)} | Q_{L_X,K_X} | \psi^{(X)} \rangle$ are independently computed multipole moments. This limit is shown as the horizontal dashed-dotted line. The remaining lines and symbols correspond to different choices for the CP procedure. Without performing a CP correction, shown as the blue dashed line, the *ab initio* points multiplied by R^n do not approach a constant, i.e., the interaction does not approach the correct asymptotic form. By contrast, the CP-corrected results smoothly approach a constant value which is in close agreement with the value obtained from independent calculations of the molecular multipole moments. This demonstrates that the long-range interaction is sensitive to the CP correction. The CP corrected results for different correction schemes are indistinguishable. This is consistent with Eq. (23), which shows that the diagonal potential is affected only by the trace of the CP correction.

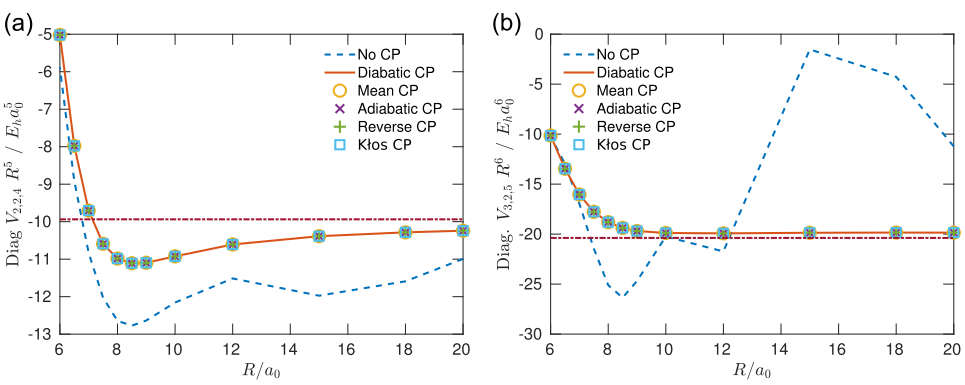

FIG. 4. Expansion coefficients of the diagonal potential for two first-order terms multiplied by R^n such that they become constant in the limit of large R. The horizontal dashed-dotted line represents the limiting value as calculated from multipole moments, whereas the other lines and symbols are obtained from *ab initio* calculations with different CP procedures, as indicated. (a) and (b) refer to L_A, L_B, L = 2, 2, 4 and 3, 2, 5, respectively.

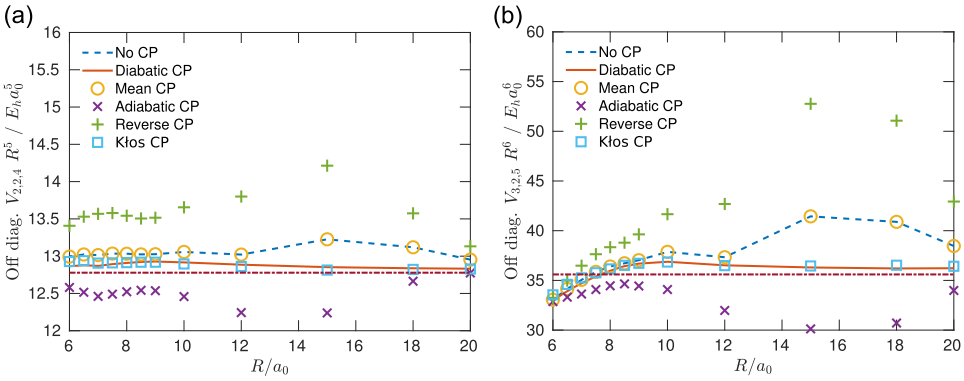

FIG. 5. Expansion coefficients of the off-diagonal potential for two first-order terms multiplied by R^n such that they become constant in the limit of large R. The horizontal dashed-dotted line represents the limiting value as calculated from multipole moments, whereas the other lines and symbols are obtained from *ab initio* calculations with different CP procedures. (a) and (b) refer to L_A, L_B, L = 2, 2, 4 and 3, 2, 5, respectively.

Figure 5 shows similar plots for the expansion coefficients of the off-diagonal potential, also for the L_A, L_B, L = 2, 2, 4 and 3, 2, 5 terms in the angular expansion. Here, we find large differences between the possible correction schemes. Again we find that the uncorrected *ab initio* points do not approach the correct long-range form. Performing a mean CP correction yields exactly the same result, which is again consistent with Eq. (23), as this correction affects only the trace of the potential energy matrix and hence only the diagonal potential. Performing the CP correction either adiabatically or reverse adiabatically also does not lead to the correct R-dependence. Finally, the method of Kłos[24] and the diabatic CP correction[33] do lead to the correct R-dependence and are in excellent agreement with the long-range theory.

C. Asymptotic diabatization

Here, we further investigate the accuracy of the asymptotic diabatization proposed in Sec. III D. Figure 6 shows several expansion terms of the off-diagonal potential using the full property-based diabatization (solid lines) and the asymptotic form (dashed lines). Full diabatization uses the multiple-property-based diabatization algorithm of Ref. 20. For diagonal terms, which are not shown, the two approaches yield identical results, as explained in Sec. III D. The leading off-diagonal term L_A, L_B, L = 2, 2, 4 is accurately reproduced by the asymptotic diabatization, with some deviations in the short range, for $R < 7a_0$. Especially the smaller terms deviate strongly in the short range.

Figure 6(b) shows the long-range behavior of the expansion coefficients multiplied by R^n. The leading term is accurately reproduced using the asymptotic transformation. It may be somewhat surprising that the next-to-leading term, $V_{3,2,5}$, comes out with the correct R dependence but a c_6 coefficient that is in error by about 20%. This is explained by writing the off-diagonal potential as

$$\langle \Pi_{+1}|\hat{V}|\Pi_{-1}\rangle = \frac{\Delta E}{2} e^{2i\varphi}, \tag{25}$$

where both the splitting of the adiabatic states, ΔE, and the mixing angle, φ, depend on the geometry. By *assuming* that the mixing angle follows its asymptotic form, we are modifying the angular dependence of the off-diagonal potential, which will affect the angular expansion coefficients. We confirm this effect by re-calculating the expansion after modifying the complex phase for a model potential containing only the first-order quadrupole-quadrupole and octupole-quadrupole interactions, with multipole moments for NO–H_2. This is seen to decrease $V_{3,2,5}$ by about 20% and to increase $V_{2,2,3}$ by about 6 a.u. We stress that the observed error is on the order of R^{-6} and hence using the asymptotic form of the mixing angle does yield the correct asymptotic interaction, which varies as R^{-5}, as expected.

This result also implies that the computation of long-range coefficients for the next-to-leading term of the off-diagonal potential represents a stringent test of diabatization algorithms: Using the asymptotic mixing angle leads to significant and constant (R-independent) errors in long-range coefficients even though the mixing angle approaches its asymptotic value arbitrarily closely. For the particular case of NO–H_2 at R = 20 a_0, we find that the difference between the asymptotic and the numerically determined mixing angles is usually on the order of 1°, with exceptions where the difference exceeds 5° in 5% of the orientations considered. Still, the property-based diabatization algorithm finds a value for c_6 which is in agreement with independently computed multipole moments better than 2%.

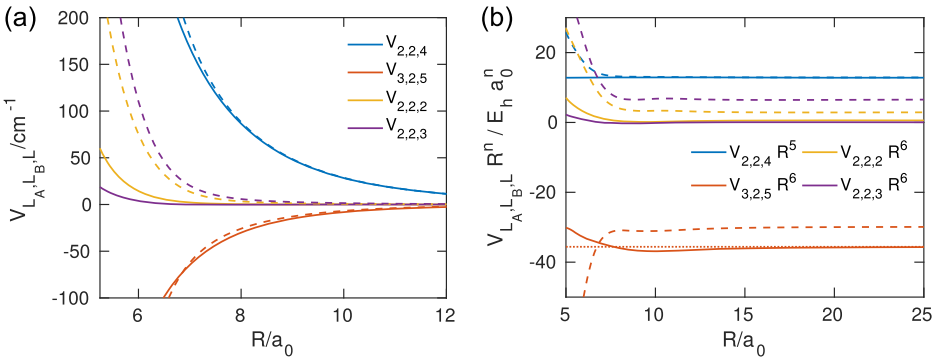

FIG. 6. (a) contains selected expansion coefficients of the off-diagonal potential using the full diabatization (solid lines) and asymptotic diabatization (dashed lines). Full diabatization uses the multiple-property-based diabatization algorithm of Ref. 20. Expansion coefficients in (b) are multiplied by R^n such that they become constant in the limit of large R.

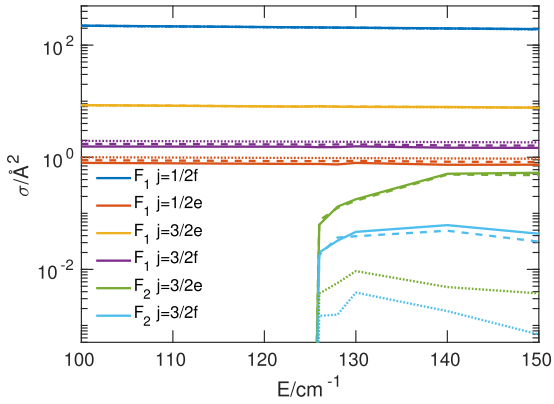

FIG. 7. Integral scattering cross sections as a function of the collision energy. Colors correspond to final states as indicated in the legend. Solid lines correspond to cross sections obtained using the fully diabatized potential, whereas dashed lines have been obtained using the asymptotic diabatization proposed here, and dotted lines correspond to the crude approximation, Eq. (11), neglecting the off-diagonal potential. Full diabatization was performed using the multiple-property-based diabatization algorithm of Ref. 20.

As discussed above, the expansion coefficients for the off-diagonal potential obtained using asymptotic diabatization are different from those obtained from full multiple-property-based diabatization precisely because both potentials are related by a geometry-dependent unitary transformation. This transformation asymptotically approaches unity in the long range and differs strongly from unity only in the short range, where the intermolecular interaction has lifted the degeneracy of the adiabatic states. It is expected that the dynamics becomes adiabatic in the short range, where the splitting is large, and hence are insensitive to this unitary transformation. To rigorously test this idea for the first time, we have performed coupled-channel scattering calculations for NO colliding with ortho H_2.

The monomer states of the NO($X^2\Pi$) molecule are labeled by the angular momentum quantum number, j_{NO}, parity e or f, and spin-orbit manifold F_1 or F_2. The ground spin-orbit state, F_1, corresponds to a bond-referred angular momentum projection quantum number $\Omega = 1/2$, whereas the excited manifold, F_2, corresponds to $\Omega = 3/2$. The hydrogen states are labeled by the angular momentum j_{H_2} and display no further fine structure. As the initial state, we consider F_1, $j_{NO} = 1/2$, f and $j_{H_2} = 1$. The channel basis contains all functions with NO total angular momenta $j_{NO} \leq 13/2$, $j_{H_2} = 1$, and total angular momentum $J \leq 81/2$. The equidistant radial grid extends from $R = 4.5$ to 40 a_0 in steps of 0.14 a_0. A detailed discussion of the time-independent scattering calculations can be found in Ref. 17.

Figure 7 shows integral cross sections for transitions to the NO $j_{NO} = 1/2$ and 3/2 states as a function of the collision energy. At an energy of approximately 124 cm^{-1}, transitions to the excited spin-orbit manifold, the F_2 states, become energetically allowed. Cross sections to these states are smaller and much more sensitive to the off-diagonal potential. Especially for these cross sections, the difference between the full multiple-property-based diabatization and asymptotic diabatization is visible on the scale of Fig. 7. In this figure, we also include the predictions based on the crude approximation, Eq. (11), of neglecting the splitting of adiabatic states or equivalently the off-diagonal potential and using only the mean potential which is independent of the mixing angle. The resulting integral cross sections are qualitatively incorrect for the spin-orbit changing transitions (F_2), but the agreement is close for purely rotational transitions (F_1). We do not recommend the crude approximation because it is outperformed by asymptotic diabatization, which is almost as simple to implement. However, the cross sections obtained in the crude approximation do indicate that rotationally

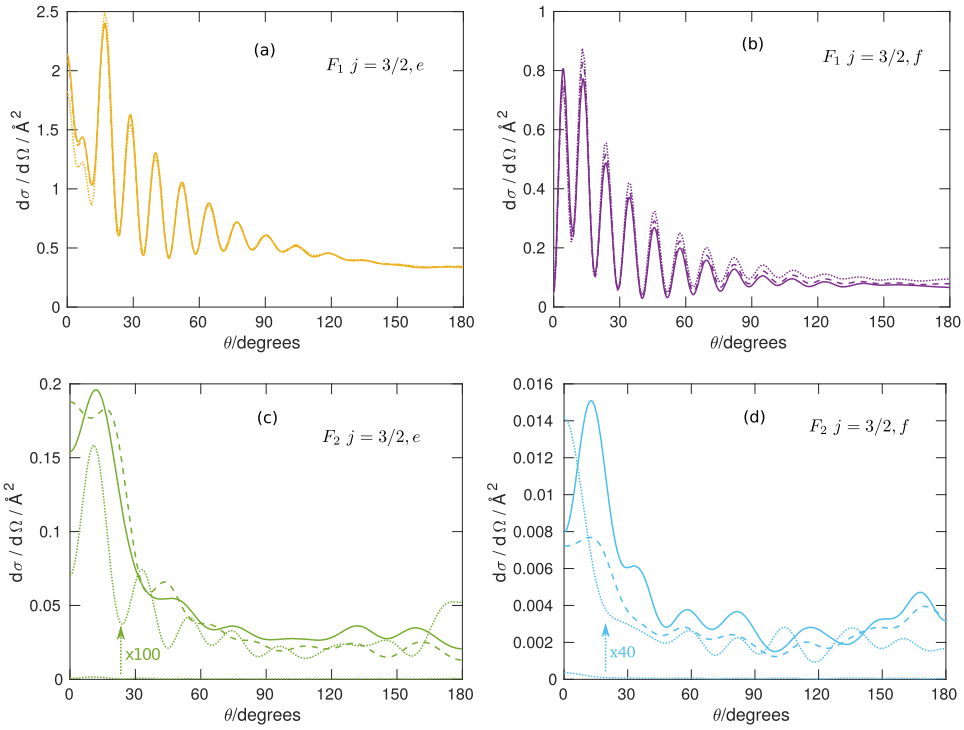

FIG. 8. Differential scattering cross sections at $E = 150\,cm^{-1}$ as a function of the scattering angle. The four panels correspond to four final states as indicated. Solid lines correspond to cross sections obtained using the fully diabatized potential, whereas dashed lines have been obtained using the asymptotic diabatization proposed here. Dotted lines correspond to the crude approximation, Eq. (11), neglecting the off-diagonal potential, magnifications of which are included in (c) and (d), as indicated. Full diabatization was performed using the multiple-property-based diabatization algorithm of Ref. 20.

inelastic cross sections are not only less sensitive to the diabatization but also insensitive to the off-diagonal potential altogether.

Figure 8 shows the differential cross sections for the transitions to $j = 3/2$ states as a function of the scattering angle, both for the rotationally (F_1) and spin-orbit (F_2) inelastic transitions. For the purely rotational transitions, the agreement between the results obtained with full multiple-property-based diabatization and asymptotic diabatization is excellent. Differences with the crude approximation are small but visible. For the more sensitive spin-orbit changing transitions, deviations between full and asymptotic diabatization are clearly visible although both the magnitude and angular dependence of the cross section are qualitatively reproduced well using the approximate asymptotic diabatization. It should be possible to resolve these differences experimentally[36–40] and hence probe nonadiabatic coupling by measuring differential cross sections for spin-orbit changing transitions. For spin-orbit changing transitions, predictions using the crude approximation are off by one or two orders of magnitude, and the angular dependence differs significantly.

VI. CONCLUSIONS

In this paper, we have revisited the theory of weakly interacting open-shell molecules. We specifically focussed on the effect of asymptotically degenerate states, which lead to significant nonadiabatic coupling. We have presented a thorough derivation of nonadiabatic couplings and their elimination by a proper choice of rotational wave functions. This leads to results that are commonly used without derivation. We showed numerically that the multiple-property-based diabatization algorithm of Ref. 20 accurately represents nonadiabatic couplings for NO($X^2\Pi$)–H_2, by comparing with numerically calculated derivative couplings of adiabatic wave functions.

We have investigated generalizations of the counterpoise procedure of Boys and Bernardi to open-shell systems.[32] We have shown that these corrections are important for obtaining the correct R-dependence of the long-range interactions. The correction to the diagonal potential is insensitive to the choice of transformation applied to the CP correction. By contrast, the off-diagonal potential is sensitive to such choices. Counterpoise corrections at the adiabatic level are shown to be inaccurate. The diabatic correction of Alexander[33] and the correction of Kłos *et al.*[24] are shown to agree well and lead to the correct long-range interactions as computed from multipole moments obtained separately from finite-field calculations. The agreement between the methods may have been surprising given that the method of Ref. 24 was presented as an adiabatic CP correction, and these are shown to perform poorly. We present a re-formulation of this method, clearly demonstrating its relation to the diabatic CP correction of Ref. 33.

We have also considered approximate diabatization by using the asymptotic transformation between adiabatic and diabatic states. This transformation is determined from long-range theory analytically and hence is straightforward to implement. This transformation removes nonadiabatic coupling asymptotically, where the adiabatic states are nearly degenerate. Residual nonadiabatic coupling does exist in the short range but should affect the dynamics to a lesser extent as the adiabatic states should be well-separated in this region. For rotationally and spin-orbit inelastic scattering of NO with $H_2(j = 1)$, we demonstrate good agreement between differential scattering cross sections using potentials obtained by full and asymptotic diabatization, respectively. Full diabatization was performed using the multiple-property-based diabatization algorithm of Ref. 20. A cruder approximation that neglects the adiabatic energy splitting performs well for pure rotational transitions, but predicted cross sections for spin-orbit inelastic scattering are off by two orders of magnitude. This method is not recommended, as it is outperformed by the appealingly simple asymptotic diabatization algorithm, and multiple-property-based diabatization can be used to more accurately represent nonadiabatic couplings.

APPENDIX: NONADIABATIC COUPLING

In this appendix, we define the monomer eigenstates, introduce the rotation-translation operator formalism, and discuss the occurrence of nonadiabatic coupling between asymptotically degenerate states. Products of monomer states are intuitively assumed to be diabatic as they depend smoothly on the nuclear coordinates. However, to the best of our knowledge, this has not been discussed rigorously in the literature. The absence of a rigorous derivation has led to the paradoxical statement that for diatomic molecules $\hat{j}_z$-adapted wave functions are diabatic, whereas their real-valued Cartesian counterparts are not even though the transformation that relates them is geometry independent.

1. Monomer states of diatomic molecules

Monomer electronic wave functions are defined as eigenstates of the monomer electronic Hamiltonian

$$\hat{H}^{(z)}_{\text{electronic}} |\psi \Lambda S \Sigma \Omega^{(z)}\rangle = \epsilon_\psi |\psi \Lambda S \Sigma \Omega\rangle^{(z)}. \tag{A1}$$

Here, ψ is the electronic state, S is the total electron spin, Λ, the bond-axis projections of the orbital, Σ, spin, and $\Omega = \Lambda + \Sigma$, total electronic angular momentum. The superscript, z, denotes that the diatomic molecule is chosen along the quantization axis. This affects the electronic Hamiltonian, $\hat{H}^{(z)}_{\text{electronic}}$, which parametrically depends on the nuclear coordinates. If the molecule is oriented at polar angles β and α, assuming the nuclear center of mass lies at the origin, the electronic Hamiltonian is given by

$$\hat{H}_{\text{electronic}} = \hat{\mathcal{R}}(\alpha, \beta, 0) \hat{H}^{(z)}_{\text{electronic}} \hat{\mathcal{R}}^\dagger(\alpha, \beta, 0), \tag{A2}$$

where the rotation operator is given by

$$\hat{\mathcal{R}}(\alpha, \beta, \gamma) = e^{-i\alpha \hat{j}_z} e^{-i\beta \hat{j}_y} e^{-i\gamma \hat{j}_z} \tag{A3}$$

with $\hat{\boldsymbol{j}}$ being the total electronic angular momentum. The monomer electronic wave functions are given by

$$|\psi \Lambda S \Sigma \Omega\rangle = \hat{\mathcal{R}}(\alpha, \beta, 0) |\psi \Lambda S \Sigma \Omega\rangle^{(z)}. \tag{A4}$$

Now, it is a standard result in the literature that Hund's case (a) rotation-electronic wave functions can be obtained as products of complex-conjugate Wigner D-matrix elements and electronic wave functions,[6]

$$|\psi\Lambda S\Sigma JM\Omega\rangle = \sqrt{\frac{2J+1}{4\pi}} D^{(J)*}_{M,\Omega}(\alpha,\beta,0)|\psi\Lambda S\Sigma\Omega\rangle\,, \tag{A5}$$

where the electronic state is usually implicit in the notation used in the literature. In what follows, we derive the action of the rotational kinetic energy on Hund's case (a) wave functions, using only the elementary angular momentum algebra of the rotation operator formalism of Ref. 50.

2. Angular derivative couplings

Here, we consider the nonadiabatic coupling due to derivatives with respect to the z-y-z Euler angles that arise from the action of rigid-body angular momentum operators, $\hat{\mathcal{J}}(\alpha,\beta,\gamma)$, see Eqs. (8)–(10) of Ref. 50, on the monomer wave functions of Eq. (A5). The nuclear angular momentum operator, $\hat{\boldsymbol{R}}$, for a diatomic molecule with polar angles (β,α) differs from the standard rigid-body angular momentum operators only by dropping terms involving the third Euler angle, γ, from the final equations. Furthermore, it is useful to introduce the body-fixed angular momentum operators $\hat{\boldsymbol{\mathcal{P}}} = \hat{\mathcal{R}}\hat{\mathcal{J}}\hat{\mathcal{R}}^{\dagger}$. The action of these operators on the electronic rotation operator of Eq. (A3) is particularly simple[51]

$$\left[\hat{\boldsymbol{\mathcal{P}}}, \hat{\mathcal{R}}(\alpha,\beta,\gamma)\right] = -\hat{\mathcal{R}}(\alpha,\beta,\gamma)\hat{\boldsymbol{j}}. \tag{A6}$$

Taking matrix elements of the above result in a basis of angular momentum kets followed by complex conjugation yields the well-known action of $\hat{\boldsymbol{\mathcal{P}}}$ on $D^{(J)*}_{M,\Omega}(\alpha,\beta,\gamma)$,

$$\begin{aligned}\left[\hat{\mathcal{P}}_{\pm1}, D^{(J)*}_{M,\Omega}(\alpha,\beta,\gamma)\right] &= c_{\mp}(j,\Omega) D^{(J)*}_{M,\Omega\mp1}(\alpha,\beta,\gamma),\\ \left[\hat{\mathcal{P}}_{z}, D^{(J)*}_{M,\Omega}(\alpha,\beta,\gamma)\right] &= \Omega\, D^{(J)*}_{M,\Omega}(\alpha,\beta,\gamma),\end{aligned} \tag{A7}$$

with, in the Condon and Shortley phase convention,

$$c_{\pm}(j,\Omega) = \sqrt{j(j+1) - \Omega(\Omega\pm1)}. \tag{A8}$$

Combining the above results, we obtain

$$\begin{aligned}\left[\hat{\mathcal{P}}_{\pm1}, D^{(J)*}_{M,\Omega}(\alpha,\beta,\gamma)\hat{\mathcal{R}}(\alpha,\beta,\gamma)\right] &= c_{\mp}(j,\Omega) D^{(J)*}_{M,\Omega\mp1}(\alpha,\beta,\gamma)\hat{\mathcal{R}}(\alpha,\beta,\gamma) - D^{(J)*}_{M,\Omega}(\alpha,\beta,\gamma)\hat{\mathcal{R}}(\alpha,\beta,\gamma)\hat{j}_{\pm1},\\ \left[\hat{\mathcal{P}}_{z}, D^{(J)*}_{M,\Omega}(\alpha,\beta,\gamma)\hat{\mathcal{R}}(\alpha,\beta,\gamma)\right] &= D^{(J)*}_{M,\Omega}(\alpha,\beta,\gamma)\hat{\mathcal{R}}(\alpha,\beta,\gamma)\left(\Omega - \hat{j}_z\right).\end{aligned} \tag{A9}$$

Using the following relation,

$$D^{(J)*}_{M,\Omega}(\alpha,\beta,0)\hat{\mathcal{R}}(\alpha,\beta,0)\,|\psi\Lambda S\Sigma\Omega\rangle^{(z)} = D^{(J)*}_{M,\Omega}(\alpha,\beta,\gamma)\hat{\mathcal{R}}(\alpha,\beta,\gamma)\,|\psi\Lambda S\Sigma\Omega\rangle^{(z)}\,, \tag{A10}$$

we find for the action on Hund's case (a) wave functions

$$\begin{aligned}\hat{R}^2\,|\psi\Lambda S\Sigma JM\Omega\rangle =& \hat{\mathcal{P}}^2\,|\psi\Lambda S\Sigma JM\Omega\,\rangle = D^{(J)*}_{M,\Omega}(\alpha,\beta,0)\hat{\mathcal{R}}(\alpha,\beta,0)\left[J(J+1) + \hat{j}^2 - 2\Omega^2\right]\,|\,\psi\Lambda S\Sigma\Omega\rangle^{(z)}\\ &- c_{+}(j,\Omega) D^{(J)*}_{M,\Omega+1}(\alpha,\beta,0)\hat{\mathcal{R}}(\alpha,\beta,0)\hat{j}_{+1}\,|\,\psi\Lambda S\Sigma\Omega\rangle^{(z)} - c_{-}(j,\Omega) D^{(J)*}_{M,\Omega-1}(\alpha,\beta,0)\hat{\mathcal{R}}(\alpha,\beta,0)\hat{j}_{-1}\,|\,\psi\Lambda S\Sigma\Omega\rangle^{(z)}\,.\end{aligned} \tag{A11}$$

This is a familiar result, and the individual terms are readily understood by writing the nuclear angular momentum as the difference of the total and electronic angular momentum. This gives $\hat{R}^2 = \hat{J}^2 + \hat{j}^2 - 2\hat{\boldsymbol{j}}\cdot\hat{\boldsymbol{J}}$, leading to the observed diagonal and Ω-uncoupling terms.

The above result has been known in the literature and has been derived using straightforward but tedious application of the chain rule of differentiation[52–55] as well as using more elegant angular momentum theoretical approaches.[50] That is, it has been shown that the use of $\hat{j}_z$-adapted electronic states combined with Wigner D-matrix elements as rotational wave functions is *sufficient* to eliminate nonadiabatic coupling.[56] It has been stated, but to our knowledge never properly discussed, whether this is actually *necessary*. The presented derivation makes explicit use of the $\hat{j}_z$-adaptation of the electronic states in Eq. (A10). If one were to repeat the derivation without this assumption, one should make use of the generally valid relation

$$D^{(J)*}_{M,K}(\alpha,\beta,0)\hat{\mathcal{R}}(\alpha,\beta,0) = D^{(J)*}_{M,K}(\alpha,\beta,\gamma)\hat{\mathcal{R}}(\alpha,\beta,\gamma)e^{i(\hat{j}_z-K)\gamma}. \tag{A12}$$

Application of the body-fixed angular momentum operators to the exponential gives rise to additional terms

$$\begin{aligned}\left[\hat{\mathcal{P}}_{\pm1}, e^{i(\hat{j}_z-K)\gamma}\right] &= \cot(\beta)\left(\hat{j}_z - K\right)e^{i(\hat{j}_z-K\mp1)\gamma},\\ \left[\hat{\mathcal{P}}_{z}, e^{i(\hat{j}_z-K)\gamma}\right] &= \left(\hat{j}_z - K\right)e^{i(\hat{j}_z-K)\gamma}.\end{aligned} \tag{A13}$$

These terms vanish only when applied to an eigenstate of $\hat{j}_z$ and the body-referred index, K, is chosen equal to that eigenvalue. If a different choice is made, the occurrence of $\cot(\beta)$ above leads to singular derivative couplings.

The analysis above explains a paradoxal statement often found in the literature, namely, that the complex $\hat{j}_z$-adapted electronic wave functions are diabatic, whereas the Cartesian components are not.[47] This cannot strictly be true, as these sets of state are related by a geometry-independent unitary transformation, so either both sets must be diabatic or they both are not. The derivation above shows that, in fact, they both lead to singular nonadiabatic couplings, but for the complex $\hat{j}_z$-adapted states, the derivative coupling is diagonal such that the singularity may be removed exactly by the right choice of rotational wave function, i.e. $K = \Omega$.

3. Translational derivative couplings

In case the nuclear center of mass is not centered at the origin of the coordinate system, the electronic wave function may be written as[57]

$$|\psi\Lambda S\Sigma\Omega\rangle = \hat{\mathcal{T}}(\boldsymbol{R}_{\rm nuc})\hat{\mathcal{R}}(\alpha,\beta,0)|\psi\Lambda S\Sigma\Omega\rangle^{(z)}. \tag{A14}$$

The electronic translation operator is given by

$$\hat{\mathcal{T}}(\boldsymbol{R}_{\rm nuc}) = e^{-i\boldsymbol{R}_{\rm nuc}\cdot\hat{\boldsymbol{p}}}, \tag{A15}$$

where $\hat{\boldsymbol{p}}$ is the electronic linear momentum operator. Nonadiabatic couplings due to the kinetic energy of the nuclear center of mass can be evaluated analogously to the angular derivative couplings above using

$$\left[\hat{\boldsymbol{P}}_{\rm nuc}, \hat{\mathcal{T}}(\boldsymbol{R}_{\rm nuc})\right] = -\hat{\mathcal{T}}(\boldsymbol{R}_{\rm nuc})\hat{\boldsymbol{p}}. \tag{A16}$$

This means that the derivative couplings with respect to the *nuclear* center of mass are non-zero although couplings due to kinetic energy of the *total* center of mass vanish exactly

$$\left[\hat{\boldsymbol{p}} + \hat{\boldsymbol{P}}_{\rm nuc}, \hat{\mathcal{T}}(\boldsymbol{R}_{\rm nuc})\right] = \hat{\mathcal{T}}(\boldsymbol{R}_{\rm nuc})(\hat{\boldsymbol{p}} - \hat{\boldsymbol{p}}) = 0. \tag{A17}$$

This is consistent with the fact that the motion of the center of mass, and not the nuclear center of mass, decouples from the internal coordinates. As we are employing electronic wave functions calculated for a fixed nuclear center of mass, we cannot exactly decouple the total center of mass. This leads to residual coupling on the order of m_e/M. The second derivative with respect to $\boldsymbol{R}_{\rm nuc}$ leads to terms proportional to $\hat{p}^2$ acting on the electronic wave functions. These couplings are related to mass polarization terms and the small difference between the bare and reduced mass of the electrons in a molecule with nuclei of finite mass.[58] These couplings also exist in the usual Born-Oppenheimer approximation for closed-shell systems, and their neglect should be an approximation of comparable accuracy.

The first derivative with respect to $\boldsymbol{R}_{\rm nuc}$ gives rise to couplings proportional to $\hat{\boldsymbol{p}}$ acting on electronic wave functions. This can be related to transition dipole moments using the operator identity

$$\hat{\boldsymbol{p}} = im_e[\hat{H}, \hat{\boldsymbol{r}}]. \tag{A18}$$

Hence, the first derivative coupling drives spurious dipole-allowed transitions.[59] These couplings for well-separated states can be eliminated by incorporating the so-called electron translation factors (ETFs).[2,59] Here, it suffices to note that the matrix elements of Eq. (A18) between degenerate eigenstates of $\hat{H}$ vanish irrespective of the dipole matrix element and hence do not give rise to additional divergent derivative couplings between the degenerate monomer states of open-shell systems. The remaining coupling to well-separated states is of the same magnitude as for the usual Born-Oppenheimer approximation in the closed-shell case.

In conclusion, we have shown that the wave functions of Eq. (A14) are diabatic in the sense that all derivative couplings, i.e., both rotational and translational, between degenerate monomer states vanish or can be eliminated by the right choice of rotational wave function. Remaining non-Born-Oppenheimer couplings to energetically well-separated states should be negligible as they are of the same order as non-Born-Oppenheimer couplings for closed-shell molecules.

[1] M. Kirste, X. Wang, H. C. Schewe, G. Meijer, K. Liu, A. van der Avoird, L. M. C. Janssen, K. B. Gubbels, G. C. Groenenboom, and S. Y. T. van de Meerakker, Science **338**, 1060 (2012).
[2] J. B. Delos, Rev. Mod. Phys. **53**, 287 (1981).
[3] S. Mahapatra, H. Köppel, and L. S. Cederbaum, J. Phys. Chem. A **105**, 2321 (2001).
[4] B. J. Rao, R. Padmanaban, and S. Mahapatra, Chem. Phys. **333**, 135 (2007).
[5] B. J. Rao, R. Padmanaban, and S. Mahapatra, J. Chem. Sci. **121**, 789 (2009).
[6] H. Klar, J. Phys. B: At., Mol. Opt. Phys. **6**, 2139 (1973).
[7] M. H. Alexander, J. Chem. Phys. **76**, 5974 (1982).
[8] W. Domcke and C. Woywod, Chem. Phys. Lett. **216**, 362 (1993).
[9] W. Domcke, C. Woywod, and M. Stengle, Chem. Phys. Lett. **226**, 257 (1994).
[10] A. J. Dobbyn and P. J. Knowles, Mol. Phys. **91**, 1107 (1997).
[11] H. Nakamura and D. G. Truhlar, J. Chem. Phys. **115**, 10353 (2001).
[12] H. Nakamura and D. G. Truhlar, J. Chem. Phys. **117**, 5576 (2002).
[13] H. Nakamura and D. G. Truhlar, J. Chem. Phys. **118**, 6816 (2003).
[14] C. E. Hoyer, X. Xu, D. Ma, L. Gagliardi, and D. G. Truhlar, J. Chem. Phys. **141**, 114104 (2014).
[15] Q. Ma, J. A. Kłos, M. H. Alexander, A. van der Avoird, and P. J. Dagdigian, J. Chem. Phys. **141**, 174309 (2014).
[16] J. A. Kłos, Q. Ma, M. H. Alexander, and P. J. Dagdigian, J. Chem. Phys. **146**, 114301 (2017).
[17] T. de Jongh, T. Karman, S. N. Vogels, M. Besemer, J. Onvlee, A. G. Suits, J. O. F. Thompson, G. C. Groenenboom, A. van der Avoird, and S. Y. T. van de Meerakker, J. Chem. Phys. **147**, 013918 (2017).
[18] Z. Gao, S. Vogels, M. Besemer, T. Karman, G. C. Groenenboom, A. van der Avoird, and S. Y. T. van de Meerakker, J. Phys. Chem. A **121**, 7446 (2017).
[19] S. N. Vogels, T. Karman, J. Kłos, M. Besemer, J. Onvlee, A. van der Avoird, G. C. Groenenboom, and S. Y. T. van de Meerakker, "Scattering resonances in bimolecular collisions between NO radicals and H_2 challenge the theoretical gold standard," Nat. Chem. (published online).
[20] T. Karman, A. van der Avoird, and G. C. Groenenboom, J. Chem. Phys. **144**, 121101 (2016).
[21] F. Rebentrost and W. A. Lester, Jr., J. Chem. Phys. **63**, 3737 (1975).
[22] F. Rebentrost and W. A. Lester, Jr., J. Chem. Phys. **64**, 3879 (1976).
[23] M. C. G. N. van Vroonhoven and G. C. Groenenboom, J. Chem. Phys. **116**, 1954 (2002).
[24] J. Kłos, G. Chałasiński, M. M. Szczęśniak, and H.-J. Werner, J. Chem. Phys. **115**, 3085 (2001).
[25] J. Kłos, G. Chałasiński, and M. M. Szczęśniak, J. Chem. Phys. **117**, 4709 (2002).
[26] R. V. Krems, G. C. Groenenboom, and A. Dalgarno, J. Phys. Chem. A **108**, 8941 (2004).
[27] T. Karman, X. Chu, and G. C. Groenenboom, Phys. Rev. A **90**, 052701 (2014).
[28] T. Karman and G. C. Groenenboom, Phys. Rev. A **90**, 052702 (2014).
[29] T. Mondal and A. J. C. Varandas, J. Chem. Phys. **135**, 174304 (2011).
[30] B. E. Applegate and T. A. Miller, J. Chem. Phys. **117**, 10654 (2002).
[31] A. van der Avoird and V. F. Lotrich, J. Chem. Phys. **120**, 10069 (2004).
[32] S. F. Boys and F. Bernardi, Mol. Phys. **19**, 553 (1970).
[33] M. H. Alexander, J. Chem. Phys. **99**, 6014 (1993).
[34] A. Thiel and H. Köppel, J. Chem. Phys. **110**, 9371 (1999).
[35] H. Köppel, J. Gronki, and S. Mahapatra, J. Chem. Phys. **115**, 2377 (2001).
[36] S. N. Vogels, J. Onvlee, A. van Zastrow, G. C. Groenenboom, A. van der Avoird, and S. Y. T. van de Meerakker, Phys. Rev. Lett. **113**, 263202 (2014).
[37] S. N. Vogels, J. Onvlee, S. Chefdeville, A. van der Avoird, G. C. Groenenboom, and S. Y. T. van de Meerakker, Science **350**, 787 (2015).
[38] J. Onvlee, A. van der Avoird, G. C. Groenenboom, and S. Y. T. van de Meerakker, J. Phys. Chem. A **120**, 4770 (2016).
[39] J. Onvlee, S. D. Gordon, S. N. Vogels, T. Auth, T. Karman, B. Nichols, A. van der Avoird, G. C. Groenenboom, M. Brouard, and S. Y. T. van de Meerakker, Nat. Chem. **9**, 226 (2016).
[40] A. von Zastrow, J. Onvlee, S. N. Vogels, G. C. Groenenboom, A. van der Avoird, and S. Y. T. van de Meerakker, Nat. Chem. **6**, 216 (2014).
[41] H. Köppel, W. Domcke, and L. S. Cederbaum, Adv. Chem. Phys. **57**, 59 (1984).
[42] M. Born and R. Oppenheimer, Ann. Phys. **389**, 457 (1927) [Ann. Phys. IV **84**, 457 (1927)].
[43] C. Xie, D. R. Yarkony, and H. Guo, Phys. Rev. A **95**, 022104 (2017).

[44]T. Karman, A. van der Avoird, and G. C. Groenenboom, J. Chem. Phys. **147**, 084306 (2017).
[45]C. A. Mead and D. G. Truhlar, J. Chem. Phys. **77**, 6090 (1982).
[46]P. J. Dagdigian, J. Chem. Phys. **145**, 114301 (2016).
[47]P. E. S. Wormer, J. A. Kłos, G. C. Groenenboom, and A. van der Avoird, J. Chem. Phys. **122**, 244325 (2005).
[48]G. C. Groenenboom, X. Chu, and R. V. Krems, J. Chem. Phys. **126**, 204306 (2007).
[49]H.-J. Werner and P. J. Knowles, with contributions from R. D. Amos, A. Berning, D. L. Cooper, M. J. O. Deegan, A. J. Dobbyn, F. Eckert, C. Hampel, T. Leininger, R. Lindh, A. W. Lloyd, W. Meyer, M. E. Mura, A. Nicklaß, P. Palmieri, K. Peterson, R. Pitzer, P. Pulay, G. Rauhut, M. Schütz, H. Stoll, A. J. Stone, and T. Thorsteinsson, MOLPRO version 2012.1, a package of *ab initio* programs, 2012, see http://www.molpro.net.
[50]G. C. Groenenboom and A. van der Avoird, "Rotation operator formalism for open shell complexes," in *Quantum Dynamics at Conical Intersections*, edited by S. C. Althorpe and G. A. Worth (Collaborative computational project on molecular quantum dynamics (CCP6), Daresbury, United Kingdom, 2004), p. 98.
[51]L. C. Biedenharn and J. D. Louck, *Angular Momentum in Quantum Physics*, Volume 8 of Encyclopedia of Mathematics (Addison-Wesley, Reading, 1981).
[52]J. T. Hougen, J. Chem. Phys. **37**, 1433 (1962).
[53]J. K. G. Watson, Mol. Phys. **19**, 465 (1970).
[54]G. Brocks, A. van der Avoird, B. T. Sutcliffe, and J. Tennyson, Mol. Phys. **50**, 1025 (1983).
[55]Y. Kim and H. Meyer, Int. Rev. Phys. Chem. **20**, 219 (2001).
[56]M. C. G. N. van Vroonhoven and G. C. Groenenboom, J. Chem. Phys. **117**, 5240 (2002).
[57]B. Zygelman, A. Dalgarno, and R. D. Sharma, Phys. Rev. A **49**, 2587 (1994).
[58]H. A. Bethe and E. E. Salpeter, "Quantum mechanics of one- and two-electron atoms," in *Handbuch der Physik* (Springer Verlag, Berlin, Germany, 1957), Vol. 35, pp. 88–436.
[59]S. Fatehi and J. E. Subotnik, J. Phys. Chem. Lett. **3**, 2039 (2012).